

Supplementary Materials for “Depth Information Assisted Collaborative Mutual Promotion Network for Single Image Dehazing”

Yafei Zhang* Shen Zhou* Huafeng Li†

Faculty of Information Engineering and Automation, Kunming University of Science and Technology

1. Parameter Selection and Analysis

In the main body of this paper, we set both parameters α and β in Eq. (1) to 1. Here, we use the SOTS-indoor dataset to analyze the effectiveness of $\alpha = 1$ and $\beta = 1$ by changing one while fixing the other. Figure 1 illustrates the PSNR curves when each parameter changes.

$$\begin{aligned} \ell_{dehaze} = & \alpha \| \mathbf{A}_{e,r} \odot (\mathbf{u}^* - \mathbf{u}) \|_1 \\ & + \beta \sum_{i=1}^n \lambda_i \frac{\| VGG_i(\mathbf{u}) - VGG_i(\Phi(\tilde{\mathbf{u}}^*, \omega_d)) \|_1}{\| VGG_i(\tilde{\mathbf{u}}^*) - VGG_i(\Phi(\tilde{\mathbf{u}}^*, \omega_d)) \|_1} \end{aligned} \quad (1)$$

It is observed from Figure 1(a) that the proposed method performs well within the range of $\alpha \in [0.75, 1.25]$, and the PSNR reaches its peak when $\alpha = 1$. Consequently, we set $\alpha = 1$. On the other hand, as shown in Figure 1(b), when β changes within $[0.75, 1.50]$, the performance is relatively high, and achieves the best when $\beta = 1$. Therefore, we set $\beta = 1$ throughout the experiment.

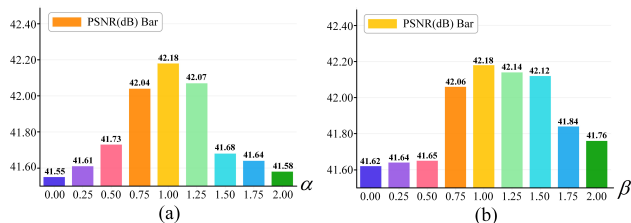


Figure 1. Parameter analysis on the SOTS-indoor dataset. PSNR curves with α and β .

2. Computational Complexity Analysis

In this section, we analyze the computational complexity of the comparative methods from three aspects: the quantity of model parameters, FLOPs, and the time required for testing. The results are listed in Table 1. The test time is the duration required for the model to process an image measuring 460×620 pixels. As indicated in Table 1, the parameter quantity

* Yafei Zhang and Shen Zhou contribute equally to this work.

† Huafeng Li (lhchina99@kust.edu.cn) is the corresponding author.

and FLOPs of our model are moderate. The test time for our model is 0.117 second, indicating a relatively fast and acceptable inference speed. Consequently, our model can be practically deployed and applied following training.

3. Experiments on Real-world Datasets

The real-world Dense-Haze [1] and NH-Haze [2] datasets are used for image dehazing in real scenarios. The Dense-Haze dataset serves as the image dehazing challenge of NTIRE2019, consisting of 55 densely hazy images with paired clear images. The NH-Haze dataset, employed in the NTIRE2020 image dehazing challenge, contains 55 pairs of non-uniformly hazy images and their corresponding clear versions. In each dataset, the last 5 images are reserved for testing, while the remaining images are used for training.

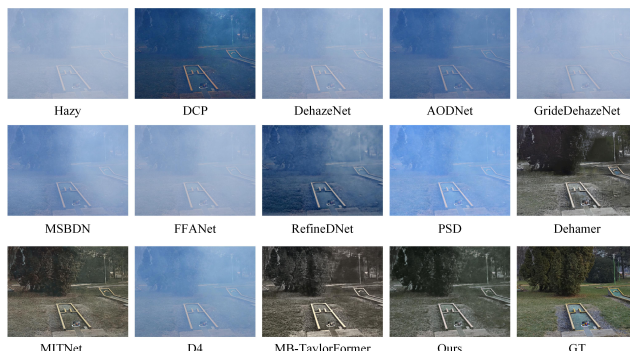


Figure 2. Visual comparison on Dense-Haze dataset.

To verify the generalizability of the proposed method, we conduct comparative experiments with existing methods on the real-world Dense-Haze and NH-Haze datasets. It is well-established that dehazing from real-world hazy images is inherently more challenging than that from synthetic hazy images. This increased difficulty stems from the typical characteristics of real-world haze, which tends to be denser and exhibits a non-uniform distribution. The dehazing results obtained by different methods on the Dense-Haze and NH-Haze datasets are shown in Figure 2 and Figure 3, respectively. From Figure 2, one can observe that

Table 1. Performance comparison of the different methods on the quantity of model parameters , FLOPs and test time.

| Methods | AECR-Net [15] | PSD [4] | MAXIM-2S [14] | Dehamer [6] | D4 [16] | Dehazeformer [13] | C2PNet [18] | MB-TaylorFormer [11] | MITNet [12] | Ours |
|---------------|---------------|---------|---------------|-------------|---------|-------------------|-------------|----------------------|-------------|-------|
| Parameters(M) | 2.61 | 6.21 | 14.10 | 135.45 | 10.7 | 25.44 | 7.17 | 7.43 | 2.49 | 7.16 |
| FLOPs(G) | 26.10 | 143.91 | 216.00 | 24.47 | 2.25 | 139.85 | 460.95 | 44.05 | 17.13 | 62.89 |
| Test time (s) | 0.006 | 0.559 | 0.641 | 0.170 | - | 0.328 | 0.929 | 1.163 | 0.049 | 0.117 |

Table 2. Performance of the proposed method is compared with that of state-of-the-art methods on real-world datasets (Dense-Haze and NH-Haze). Best values are in bold.

| Methods | Dense-Haze | | | | | NH-Haze | | | | |
|----------------------|--------------|---------------|---------------|---------------|---------------|--------------|---------------|---------------|---------------|---------------|
| | PSNR↑ | SSIM↑ | NIQE↓ | PIQE↓ | FADE↓ | PSNR↑ | SSIM↑ | NIQE↓ | PIQE↓ | FADE↓ |
| DCP [7] | 11.01 | 0.4165 | 5.2502 | 15.0944 | 2.7647 | 10.57 | 0.5196 | 5.2502 | 5.0944 | 0.7647 |
| DehazeNet [3] | 9.48 | 0.4383 | 6.5778 | 7.9937 | 2.6119 | 16.62 | 0.5238 | 2.8354 | 5.2104 | 0.6675 |
| AOD-Net [8] | 12.82 | 0.4683 | 6.2253 | 10.3068 | 1.9741 | 15.40 | 0.5693 | 2.8416 | 5.5681 | 0.3620 |
| GridDehazeNet [9] | 14.96 | 0.5326 | 7.0555 | 10.7274 | 4.3710 | 10.07 | 0.3986 | 2.8246 | 5.6275 | 0.7486 |
| MSBDN [5] | 15.13 | 0.5551 | 6.6765 | 9.8121 | 3.1787 | 19.23 | 0.7056 | 2.6862 | 5.2017 | 0.7423 |
| FFA-Net [10] | 12.22 | 0.4440 | 6.8754 | 20.1206 | 1.1549 | 19.87 | 0.6915 | 2.6624 | 5.7624 | 1.0356 |
| RefineDNet [17] | 12.91 | 0.4584 | 5.8663 | 11.4998 | 1.1159 | 12.91 | 0.4584 | 2.8067 | 5.9807 | 0.4605 |
| PSD [4] | 9.73 | 0.4345 | 5.4040 | 10.9304 | 1.6434 | 10.32 | 0.5274 | 2.8556 | 5.0698 | 0.4563 |
| Dehamer [6] | 16.22 | 0.5602 | 6.5784 | 56.5955 | 1.3626 | 20.66 | 0.6844 | 2.9575 | 8.0992 | 0.3883 |
| D4 [16] | 11.49 | 0.4821 | 6.1627 | 14.8036 | 2.2183 | 12.66 | 0.5072 | 2.5849 | 5.7850 | 0.5359 |
| Dehazeformer [13] | 16.29 | 0.5100 | - | - | - | 20.47 | 0.7310 | - | - | - |
| C2PNet [18] | 16.88 | 0.5728 | - | - | - | - | - | - | - | - |
| MB-TaylorFormer [11] | 16.44 | 0.5660 | 5.8181 | 21.1580 | 1.1907 | - | - | - | - | - |
| MITNet [12] | 16.97 | 0.6056 | 6.0711 | 35.8864 | 1.8673 | 21.26 | 0.7122 | 3.0026 | 10.1390 | 0.3624 |
| Proposed | 17.00 | 0.6101 | 5.1017 | 6.7368 | 1.0696 | 20.46 | 0.7963 | 2.5186 | 4.9142 | 0.3535 |

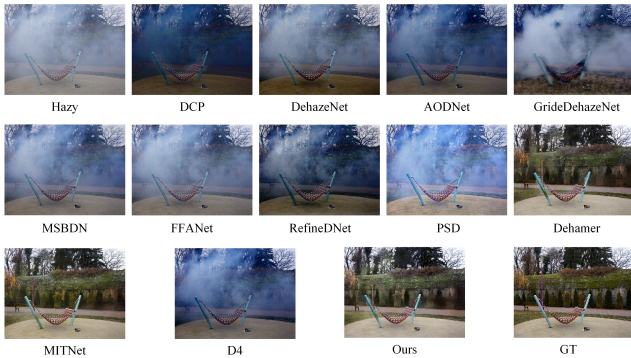


Figure 3. Visual comparison on NH-Haze dataset.

on the Dense-Haze dataset, the dehazing results of compared methods is not satisfactory except Dehamer, MB-TaylorFormer, MITNet and the proposed method. However, those four methods mentioned above provide limited dehazing outcomes for dense haze, where the haze residues and color distortion still exist to some extent. From Figure 3, it can be seen that the dehazing results are poor on NH-Haze dataset, with the exception of Dehamer, MITNet and the proposed method.

Furthermore, the quantitative evaluation results on the Dense-Haze and NH-Haze datasets are presented in Table 2. It can be seen that the proposed method achieves the best values across all evaluation metrics when applied to the

Dense-Haze dataset. For the NH-Haze dataset, the proposed method attains either the best or comparable scores on the evaluation metrics. The experimental results demonstrates the effectiveness of proposed method and its superiority over the state-of-the-art methods.

4. Additional Dehazing Results on Real-world Images

To further validate the generalizability of the proposed model, we present the dehazing results of different methods on real-world dense hazy images, as shown in Figure 4. From Figure 4, it is evident that our method yields the most favorable visual results and also attains the best values in quantitative evaluation metrics.

5. Additional Dehazing Results on Synthetic Datasets

For a comprehensive comparison, we provide additional dehazing results of different methods on the SOTS-indoor and SOTS-outdoor datasets in Figure 5. Moreover, to facilitate the visual comparison, we display the difference maps between the enclosed areas and their GTs. The difference maps reveal that the proposed method yields consistently superior dehazing results compared to other methods.

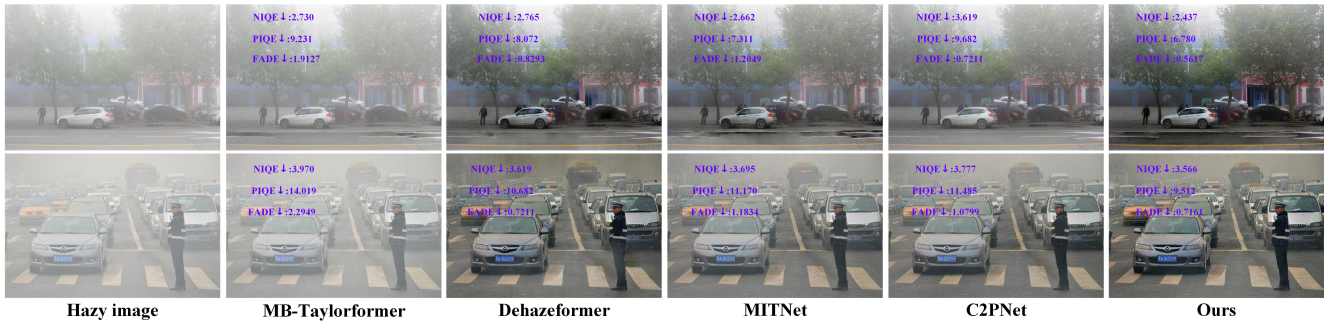


Figure 4. Visual comparison on real-world dense hazy images.

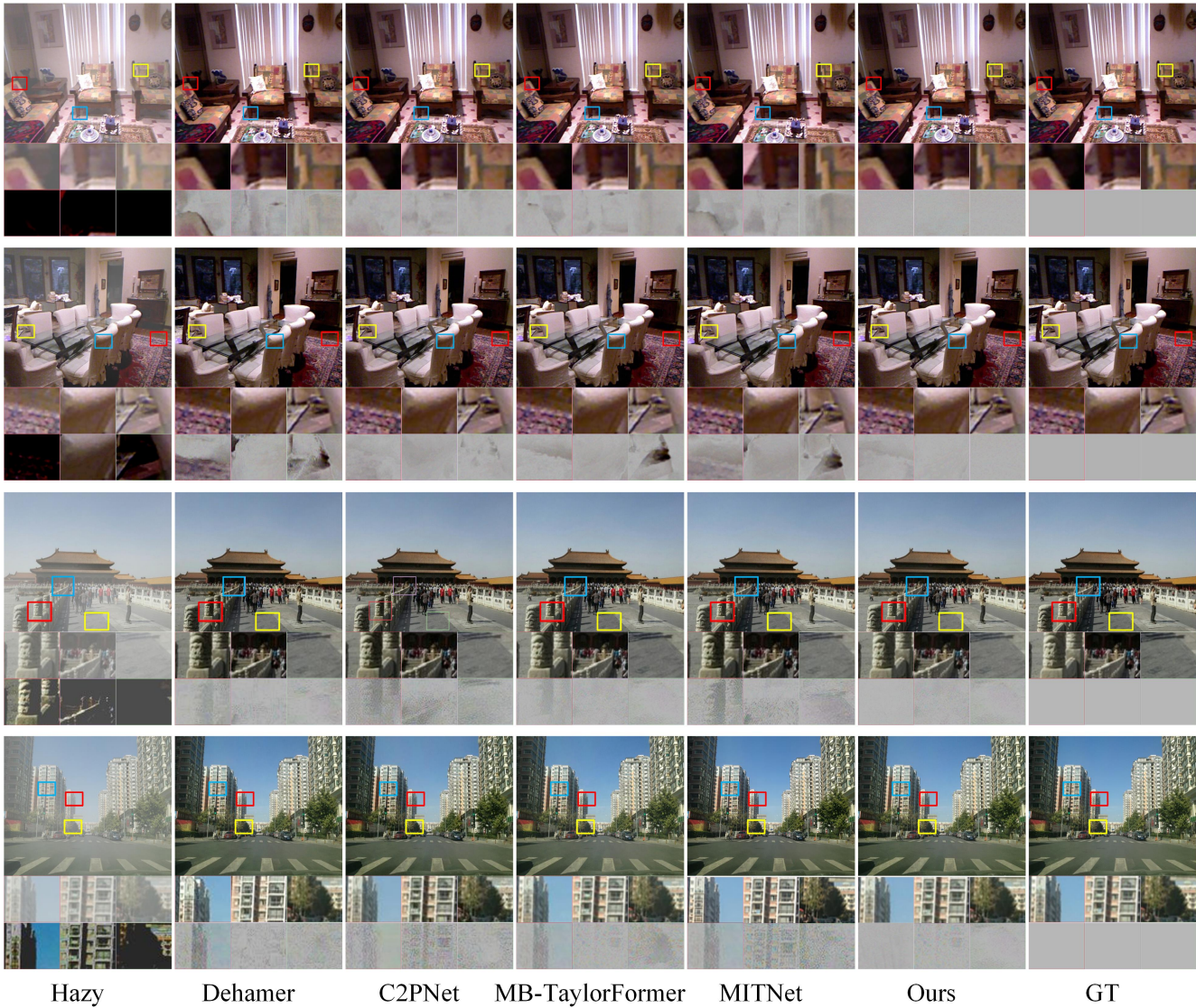


Figure 5. Additional visual comparisons on SOTS-indoor and SOTS-outdoor.

References

- [1] Codruta O. Ancuti, Cosmin Ancuti, Mateu Sbert, and Radu Timofte. Dense-haze: A benchmark for image dehazing with

dense-haze and haze-free images. In *ICIP*, pages 1014–1018, 2019. 1

- [2] Codruta O. Ancuti, Cosmin Ancuti, and Radu Timofte. Nh-haze: An image dehazing benchmark with non-homogeneous hazy and haze-free images. In *CVPRW*, pages 1798–1805, 2020. 1
- [3] Bolun Cai, Xiangmin Xu, Kui Jia, Chunmei Qing, and Dacheng Tao. Dehazenet: An end-to-end system for single image haze removal. *IEEE Transactions on Image Processing*, 25(11):5187–5198, 2016. 2
- [4] Zeyuan Chen, Yangchao Wang, Yang Yang, and Dong Liu. Psd: Principled synthetic-to-real dehazing guided by physical priors. In *CVPR*, pages 7176–7185, 2021. 2
- [5] Hang Dong, Jinshan Pan, Lei Xiang, Zhe Hu, Xinyi Zhang, Fei Wang, and Ming-Hsuan Yang. Multi-scale boosted dehazing network with dense feature fusion. In *CVPR*, pages 2154–2164, 2020. 2
- [6] Chunle Guo, Qixin Yan, Saeed Anwar, Runmin Cong, Wenqi Ren, and Chongyi Li. Image dehazing transformer with transmission-aware 3d position embedding. In *CVPR*, pages 5802–5810, 2022. 2
- [7] Kaiming He, Jian Sun, and Xiaoou Tang. Single image haze removal using dark channel prior. *IEEE Transactions on Pattern Analysis and Machine Intelligence*, 33(12):2341–2353, 2011. 2
- [8] Boyi Li, Xiulian Peng, Zhangyang Wang, Jizheng Xu, and Dan Feng. Aod-net: All-in-one dehazing network. In *ICCV*, pages 4780–4788, 2017. 2
- [9] Xiaohong Liu, Yongrui Ma, Zhihao Shi, and Jun Chen. Grid-dehazenet: Attention-based multi-scale network for image dehazing. In *ICCV*, pages 7313–7322, 2019. 2
- [10] Xu Qin, Zhilin Wang, Yuanchao Bai, Xiaodong Xie, and Huizhu Jia. Ffa-net: Feature fusion attention network for single image dehazing. In *AAAI*, pages 11908–11915, 2020. 2
- [11] Yuwei Qiu, Kaihao Zhang, Chenxi Wang, Wenhan Luo, Hongdong Li, and Zhi Jin. Mb-taylorformer: Multi-branch efficient transformer expanded by taylor formula for image dehazing. In *ICCV*, pages 12756–12767, 2023. 2
- [12] Hao Shen, Zhong-Qiu Zhao, Yulun Zhang, and Zhao Zhang. Mutual information-driven triple interaction network for efficient image dehazing. In *ACM MM*, pages 7–16, 2023. 2
- [13] Yuda Song, Zhuqing He, Hui Qian, and Xin Du. Vision transformers for single image dehazing. *IEEE Transactions on Image Processing*, 32:1927–1941, 2023. 2
- [14] Zhengzhong Tu, Hossein Talebi, Han Zhang, Feng Yang, Peyman Milanfar, Alan Bovik, and Yinxiao Li. Maxim: Multi-axis mlp for image processing. In *CVPR*, pages 5759–5770, 2022. 2
- [15] Haiyan Wu, Yanyun Qu, Shaohui Lin, Jian Zhou, Ruizhi Qiao, Zhizhong Zhang, Yuan Xie, and Lizhuang Ma. Contrastive learning for compact single image dehazing. In *CVPR*, pages 10546–10555, 2021. 2
- [16] Yang Yang, Chaoyue Wang, Risheng Liu, Lin Zhang, Xiaojie Guo, and Dacheng Tao. Self-augmented unpaired image dehazing via density and depth decomposition. In *CVPR*, pages 2027–2036, 2022. 2
- [17] Shiyu Zhao, Lin Zhang, Ying Shen, and Yicong Zhou. Refinednet: A weakly supervised refinement framework for single image dehazing. *IEEE Transactions on Image Processing*, 30:3391–3404, 2021. 2
- [18] Yu Zheng, Jiahui Zhan, Shengfeng He, Junyu Dong, and Yong Du. Curricular contrastive regularization for physics-aware single image dehazing. In *CVPR*, pages 5785–5794, 2023. 2